

Covy: An AI-powered Robot with a Compound Vision System for Detecting Breaches in Social Distancing

SERGE SAAYBI, The Delft University of Technology, The Netherlands

AMJAD YOUSEF MAJID, The Delft University of Technology, The Netherlands

R VENKATESHA PRASAD, The Delft University of Technology, The Netherlands

ANIS KOUBAA, Prince Sultan University, Saudi Arabia

CHRIS VERHOEVEN, The Delft University of Technology, The Netherlands

This paper introduces a compound vision system that enables robots to localize people up to 15 m away using a cheap camera. And, it proposes a robust navigation stack that combines Deep Reinforcement Learning (DRL) and a probabilistic localization method. To test the efficacy of these systems, we prototyped a low-cost mobile robot that we call Covy. Covy can be used for applications such as promoting social distancing during pandemics or estimating the density of a crowd. We evaluated Covy’s performance through extensive sets of experiments both in simulated and realistic environments. Our results show that Covy’s compound vision algorithm doubles the range of the used depth camera, and its hybrid navigation stack is more robust than a pure DRL-based one.

CCS Concepts: • **Human-centered computing** → **Empirical studies in ubiquitous and mobile computing**.

Additional Key Words and Phrases: Human-robot interaction, mobile robots, vision, deep reinforcement learning, covid-19

ACM Reference Format:

Serge Saaybi, Amjad Yousef Majid, R Venkatesha Prasad, Anis Koubaa, and Chris Verhoeven. 2022. Covy: An AI-powered Robot with a Compound Vision System for Detecting Breaches in Social Distancing. 1, 1 (August 2022), 15 pages. <https://doi.org/XXXXXXX.XXXXXX>

1 INTRODUCTION

Robots are becoming ubiquitous in our daily life (e.g. serving in hotels and restaurants [11], inspecting plants [31], etc.). Events like the COVID-19 pandemic have accelerated their adoption in our society. For example, robots have been proposed to encourage people to maintain safe distances and wear masks during the said pandemic [39]. Such applications pose an interesting trade-off: *mass production demands the robots to be cheap, but operating in complex environments requires them to be sophisticated, and consequently expensive*. Obviously, addressing this challenge can be done in two ways: (i) using an advanced and expensive robot (e.g., Spot [20]) and then trying to bring the cost down for production en masse; or (ii) starting with a cheap robot and then advancing it to meet the application requirements. We opted for the latter and developed *Covy* (Figure 1). Covy is equipped with the Intel RealSense D435i depth camera [21] which has a nominal range of 10 m. However, its effective range according to our experiments is about 6 m which

Authors’ addresses: Serge Saaybi, The Delft University of Technology, Delft, The Netherlands; Amjad Yousef Majid, The Delft University of Technology, Mekelweg 4, Delft, The Netherlands, a.y.majid@tudelft.nl; R Venkatesha Prasad, The Delft University of Technology, Delft, The Netherlands; Anis Koubaa, Prince Sultan University, Riyadh, Saudi Arabia; Chris Verhoeven, The Delft University of Technology, Delft, The Netherlands.

Permission to make digital or hard copies of all or part of this work for personal or classroom use is granted without fee provided that copies are not made or distributed for profit or commercial advantage and that copies bear this notice and the full citation on the first page. Copyrights for components of this work owned by others than ACM must be honored. Abstracting with credit is permitted. To copy otherwise, or republish, to post on servers or to redistribute to lists, requires prior specific permission and/or a fee. Request permissions from permissions@acm.org.

© 2022 Association for Computing Machinery.

Manuscript submitted to ACM

Manuscript submitted to ACM

1

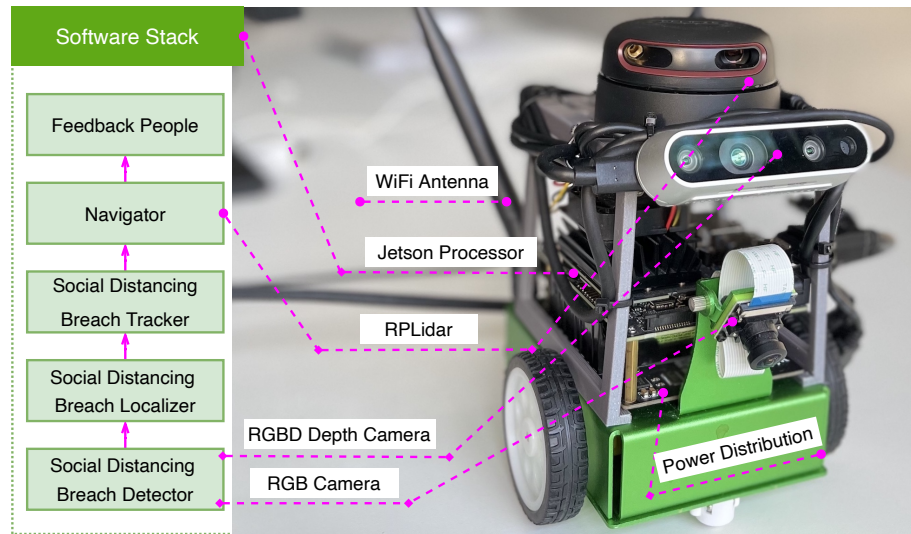


Fig. 1. Hardware and software overview of Covy: a prototype swarm robot for promoting social distancing practice.

is too limited to detect breaches in social distancing—the application that we focused on to test Covy’s vision and navigation systems. To navigate to the breachers, Covy relies on its LiDAR and a hybrid navigation stack that combines the Adaptive Monte Carlo Localization (AMCL) algorithm [4] with a DRL agent. Developing a robot like Covy poses many challenges; however, here, we only mention the ones relevant to our research focus.

Challenges. Covy was developed with two main challenges in mind:

❶ Designing a long-range, low-cost vision system that can estimate the 3D coordinates of people in the scene. The localization of nearby people must be sufficiently accuracy to enable safe human-robot interaction. ❷ AI algorithms show an excellent ability to generalize across different tasks and hardware. As such, Covy’s navigation stack should be AI-based to facilitate code portability and generalizability.

Contributions. Our contributions are manifold. ❶ We built a platform with complete stack called Covy and used it for evaluation. ❷ We developed a compound vision system that doubles the effective range of the Intel RealSense depth camera for detecting social distancing breaches. ❸ We developed a hybrid navigation stack that combines the power of Deep Reinforcement Learning and a probabilistic localization method. ❹ We evaluated Covy by conducting extensive experiments in simulated and realistic environments.

2 RELATED WORK

2.1 Technology-Driven Social Behavior Encouragement.

Encouraging desired social behaviors using robots is an emerging field of research that lies on the intersection between swarm robotics [8, 13], Artificial Intelligence (AI) [42], and human-robot interaction [3]. This emergence has been accelerated during the COVID-19 pandemic as reducing human-to-human interaction was found to be necessary to limit the spread of the virus [48, 52]. Consequently, many technological solutions have been proposed to keep our society functioning in such situations. These proposals can be generally categorized into two categories: passive and active systems.

Passive systems focus on detecting and analyzing social behaviors [2, 35, 40]. In general, these systems utilize CCTV security cameras and an object detection algorithm (e.g., YOLO [38]) to detect people in the scene. They also leverage tracking algorithms such as SORT [7] or DeepSORT [53] to keep track of the identified pedestrians across multiple frames. The obvious limitation of these systems is that they cannot provide feedback to people which is necessary to limit the spread of a virus, for example.

Active systems, on the other hand, provide feedback to users when they violate the recommended guidelines. They can be further sub-divided into end-user dependent and end-user independent systems. Smartphones and wearables are examples of end-user dependent active systems. They have been proposed to be used for maintaining safe distances from other people during COVID-19 [9, 46, 49]. However, privacy concerns discourage people from installing the needed applications which renders this option ineffective. In contrast to smartphones and wearables, robots are end-user independent systems. They can be deployed on demand to targeted locations to encourage people to follow certain recommendations. Different types of robots have been proposed to support us during the fight against the COVID-19 virus. Dr. spot is a teleoperated quadruped robot that monitors social distancing and face masking in public space and alerts offenders [46]. Chen et al. [10] introduced a fully autonomous expensive surveillance quadruped for desired social behaviors encouragement. The high prices of these robots make their large-scale deployment prohibitively expensive. Therefore, Sathyamoorthy et al. [43] proposed a low-cost robotic system – similar to Covy – able to detect and navigate towards the breaches using an RGB-D camera and 2D LiDAR. Their system also leverages static CCTV camera to increase the detection range. However, its major drawback is the limited detection range of only up to 4 m for the mounted depth camera and 3 m for the fixed CCTV camera. We, in this work, propose a compound low-cost vision system with a breach detection range of up to 16 m.

2.2 Robot Navigation.

There is a growing interest in DRL-based robotic navigation [23, 33, 50, 51]. This is driven mainly by the portability of a DRL navigation stack to different robotic platforms and its capability of online learning. Tai et al. [51] used Deep Deterministic Policy Gradient (DDPG) to develop a mapless motion planner that enables a robot to navigate unseen real environments with obstacles. Costa de Jesus et al. [12] replaced the DDPG with the Soft Actor-Critic [17] (SAC) DRL model and showed its efficacy through simulation. Long et al. [30] utilized Proximal Policy Optimization (PPO) [44] to develop a multi-robot collision avoidance policy. The PPO agent directly maps raw sensory data to steering commands. The authors validated the policy in various simulated environments. Kulhánek et al. [27] developed a camera-based navigation stack by extending a version of the batched A2C algorithm [33]. The A2C agent was deployed on a real robot for validation [26]. For Covy, we experimented with DDPG and SAC, a deterministic and probabilistic DRL model, and developed a hybrid navigation stack to overcome some of the observed limitations in a pure DRL approach.

3 SYSTEM OVERVIEW

3.1 Hardware

Figure 1 shows Covy’s hardware and software stack, which are explained next.

Main CPU.

Covy is based on the Jetson single-board computer (JSBC) family. We favored this option because (i) the JSBC family provides multiple processors with increasing CPU and GPU capabilities, and (ii) code portability between these

Table 1. The main specifications of the embedded hardware for edge AI taken into account.

Specifications	Raspberry Pi 4 + Intel Movidius	Raspberry Pi 4 + Coral Accelerator	Jetson Nano	Jetson Xavier NX
GPU	Up to 150 GFLOPS ¹	Up to 4 TOPS ² (INT8)	472 GFLOPS (FP32)	21 TOPS (INT8)
Accelerator	Broadcom Video Core VI (32-bit) + Myriad X VPU	Broadcom Video Core VI (32-bit) + Google Edge TPU coprocessor	128 CUDA cores NVIDIA Maxwell	384-core NVIDIA Volta GPU with 48 Tensor Cores
CPU	Quad-core ARM CortexA72 64-bit @ 1.5 GHz	Quad-core ARM CortexA72 64-bit @ 1.5 GHz	Quad-core ARM Cortex-A57 MPCore processor	6-core NVIDIA Carmel ARMv8.2 64-bit CPU 6MB L2 + 4MB L3
Memory	8 GB LPDDR4 + 4 GB LPDDR3	8 GB LPDDR4	4 GB 64-bit LPDDR4, 1600 MHz 25.6 GB/s	16 GB 128-bit LPDDR4x @ 1866 MHz 59.7 GB/s
Storage	Micro-SD	Micro-SD	Micro-SD or 16 GB eMMC 5.1	Micro-SD or 16 GB eMMC 5.1
Price	100 €	100 €	100 €	326 €

¹ GFLOPs: a computer system that is capable of performing one billion floating-point operations per second.

² TOPS: trillion operations per second.

processors is relatively easy. Our experiments were conducted with Jetson Nano and Jetson Xavier NX. Table 1 compares the used processors to other low-cost options.

Vision Sensor. An RGB-D camera captures RGB images and their depth information on a per-pixel basis [32]. As such it is a natural choice for estimating the 3D coordinates of objects in images. The two most suitable depth cameras for our applications are the ZED2 [47] and the Intel RealSense D435i [34]. The ZED2 has twice the depth range of the D435i but also costs twice as much. We chose to work with the lower-cost D435i which has a nominal depth range of 10 m.

Robot body. We selected the JetBot AI kit [22] for developing our robot due to its low price (≈ 300 €) and its growing usage for AI tasks [15, 24, 37]. JetBot is a differential-driven vehicle with an IMX219 8MP camera mounted to the front. It is powered by an NVIDIA processor, allowing it to run AI tasks such as facial recognition, object tracking, auto line following, and collision avoidance. As we target indoor environments we equipped JetBot with a 2D LiDAR [41] to enable it to navigate autonomously in buildings.

3.2 Software

Covy’s software architecture is divided into two main modules: breach detection and navigation. These modules are further sub-divided into several ROS (Robot Operating System) nodes [36].

3.2.1 Breach Detection. To localize people in the scene, Covy processes an image twice: first, it processes an RGB-D image to localize nearby people, and second, it analyzes only an RGB image to estimate the locations of faraway people.

RGB-D based Localization:- Covy uses YOLOv3 [1] – a real-time object detection algorithm that features 53 convolutional neural network layers with residual connections – to detect the 2D coordinates of people in the scene. YOLOv3 ROS (ROS implementation of YOLOv3) [38] takes an RGB image as input and publishes three ROS topics:

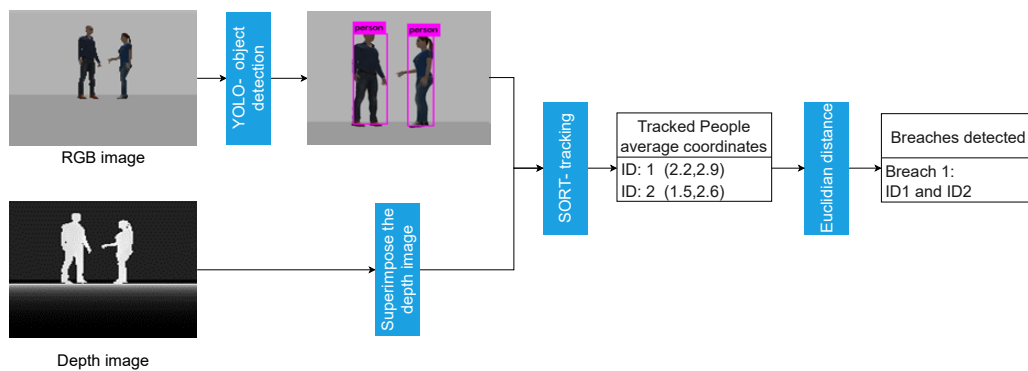


Fig. 2. The RGB-D breach detection algorithm.

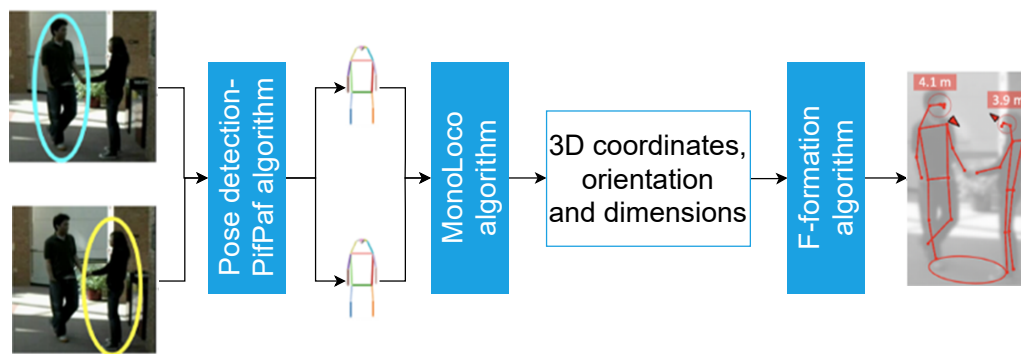


Fig. 3. An RGB breach detection algorithm [6]

bounding boxes around identified objects, their categories, and confidence scores. To determine the 3D coordinates of the identified people, Covy obtains the depth data as a point cloud from the Intel RealSense camera.

To fuse the depth data with the RGB image, the centers of the boxes surrounding people are calculated. Then the depth points closest to these centers are chosen to get the 3D coordinates of people in the image. The obtained 3D coordinates are then sent to the SORT (Simple Online and Real-time Tracking) algorithm [7] to track people across multiple images. SORT utilizes the position and size of the bounding box for motion estimation and data association using Kalman filter and the Hungarian method, respectively. Then, it outputs unique IDs for each identified pedestrian. After tracking the identified people for 20 frames, their 3D coordinates are averaged and the inter-person distance is calculated using the Euclidean distance measure. If the distance between two individuals is less than a prespecified threshold (e.g., 1.5 m) Covy reports a breach. Figure 2 visualizes the RGB-D based breach detection process. This process is repeated pairwise for all the detected individuals. The result is a list of breaches containing the different groups of non-compliant pedestrians. Covy determines the largest group, computes its middle coordinates, and sends these coordinates to the navigation module.

RGB based Localization:- Since depth information is only available at a short-range (our experiments show an effective range of 6 m), when no individuals are detected Covy switches to MonoLoco [5] for long-range scanning (i.e., up to 20 m). MonoLoco processes an RGB image as a set of 2D joints using two pose detectors: Mask R-CNN [19], which

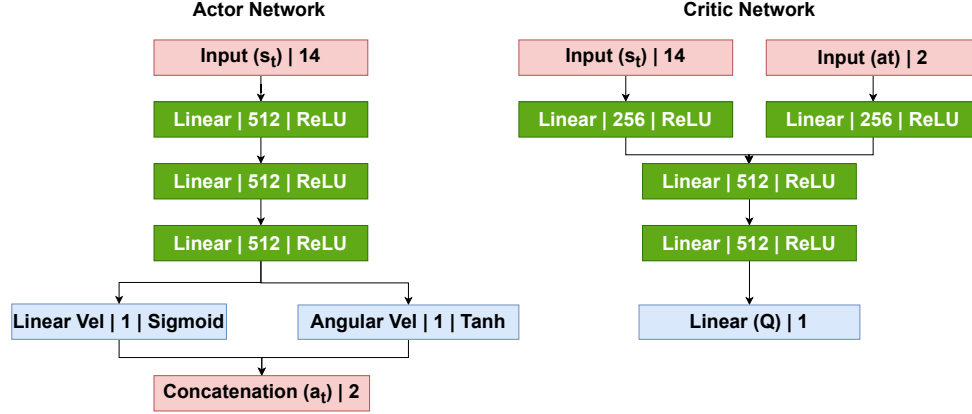


Fig. 4. DDPG network structure [51].

works top-down, and OpenPifPaf [25], which works bottom-up. The MonoLoco algorithm then takes these 2D joints as input and outputs the 3D locations, orientations, and dimensions of the detected people together with localization uncertainty. For that, the algorithm uses six fully-connected neural network (DNN) layers of 256 nodes each. The DNN uses dropout after every fully connected layer and includes batch normalization and residual connections. The output values are analyzed to discover F-formations [45]—spatial patterns constructed during interactions between two people or more—and evaluate social distancing breaches (Figure 3). Finally, the system publishes an approximation of each pedestrian’s x, y, z coordinates identified in the image along with their status as breachers or not. The navigation module then guides Covy towards the largest breach density. Using this compound procedure Covy doubles the effective range of Intel RealSense at no additional costs.

3.2.2 Navigation. We have experimented with a deterministic and probabilistic DRL algorithm to develop Covy’s navigation stack. Namely, we implemented the Deep Deterministic Policy Gradient (DDPG)[51] and Soft Actor-Critic (SAC) [12, 54] algorithm. The implementation of the said algorithms requires the definition of the state space, action space, network architecture, and reward function which we specify next.

State Space:- The environment is observed through 10 laser rays emitted by the LiDAR from -90° to 90° in front of the robot. These measurements are combined with the angular and linear velocity and the relative position and angle of the robot to the target. These values are grouped in vector to form the input state to a DRL agent.

Action Space:- Both the DDPG and SAC agents have actor-critic network architectures that act in a continuous action space [28]. The action space has two dimensions: the angular and linear velocities. The angular and linear velocities are limited to $[-2,2]$ rad/s and $[0,0.2]$ m/s for smooth navigation.

Deep Deterministic Policy Gradient Network (DDPG):- The DDPG [28] is an actor-critic DRL agent. Its actor network consists of three fully-connected neural network layers with 512 nodes each. A rectified linear unit (ReLU) activation follows each layer. The output layer produces two action parameters representing the robot’s linear and angular velocities. A hyperbolic tangent \tanh activation function is applied to the angular velocity to limit its range to $[-2,2]$ rad/s, and a sigmoid activation function keeps the range of the linear velocity within $[0,0.2]$ m/s. The critic-network takes as input a pair of a state and action vectors and outputs their associated Q value. Its architecture is similar

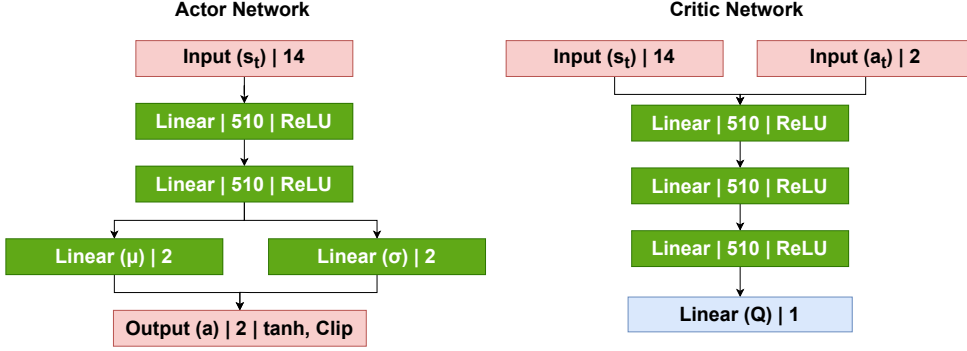


Fig. 5. SAC network structure [18, 54]. Each layer includes its type, dimension, and activation function.

to that of the actor network except for the first hidden layer which is split into two 256-neurons layers¹ (Figure 4). Our implementation of the DDPG agent is based on those proposed in [12, 51] with minor modifications to the critic network.

Soft Actor-Critic Network (SAC):- SAC consists of three networks: an actor and two critic networks. The critic networks are trained independently, and the minimum of their Q-values is then used to update the actor network [18]. The actor is composed of 2 fully connected hidden layers with 510 neurons each (Figure 5). It generates a mean and log standard deviation which are used to output the angular and linear velocities commands. A hyperbolic tangent \tanh activation function and the clip operation are applied to limit the linear and angular velocity in the range $[0, 0.2]$ m/s and $[-2, 2]$ rad/s, respectively. A critic network takes as input the current state and action and uses three fully-connected hidden layers to process the associated Q-value. Our implementation of SAC is based on [54]; however, we omitted the value network as recommended in [18].

Reward function:- A reward signal is what enables a DRL agent to learn. We used the following reward function to train our DRL agents (i.e., DDPG and SAC) to navigate to a destination in indoor environments,

$$r(s_t, a_t) = \begin{cases} r_a & \text{if } D_t < T \\ r_c & \text{if } L_t < \min_c \\ r_{d1}(D_{t-1} - D_t) & \text{if } (D_{t-1} - D_t) > 0 \\ r_{d2} & \text{if } (D_{t-1} - D_t) \leq 0 \end{cases}$$

Covy receives a large positive reward if it reaches the goal, a large negative reward if it collides², a positive reward proportional to its progress towards the goal after each steps, and a constant negative reward otherwise. Through such a reward and punishment system, the robot learns to navigate from start to destination while avoiding obstacles. Also, it learns to overcome local minima. For example, if the robot does not receive a large positive reward when reaching the goal, it may learn to crash into the nearest wall to get the smallest negative reward.

Hybrid Autonomous Navigation:- When we deployed the DRL navigation stack on the physical robot, we noticed that the LiDAR odometry—which refers to determining the robot’s position relative to its starting point using LiDAR

¹Other implementations may use a single 512 neurons layer. Based on our experiments this implementation seemed to give better performance and that is why we chose the architecture with the split first hidden layer.

²more precisely, if the LiDAR reading, L_t , is smaller than a certain minimum, \min_c , the robot is regarded to be collided and gets a large negative reward

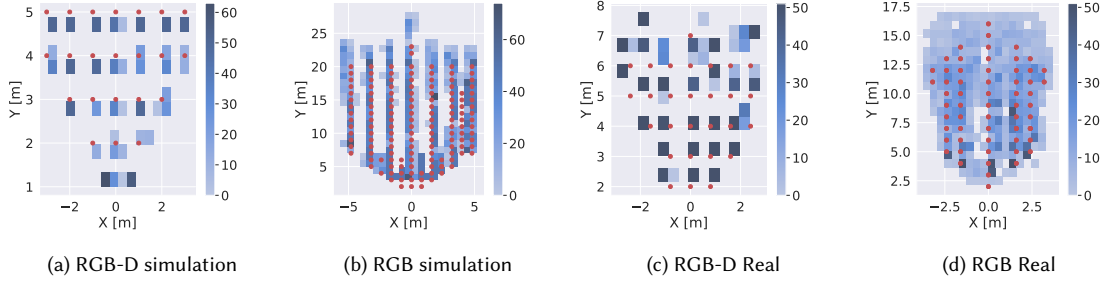


Fig. 6. Heatmap showcasing the ground truth measurements (red circles) versus the approximated ones (blue squares).

readings—often gets lost. Whenever this happens, the navigation fails and the robot is unable to reach the target. To counter this unwanted behavior, we developed a hybrid navigation stack that combines DRL and the Adaptive Monte Carlo Localization (AMCL) algorithm [14]. The AMCL is a probabilistic algorithm that localizes a robot on a given map. To recover from any failure mode that may happen due to LiDAR odometry issues, Covy obtains the robot pose estimation from AMCL and compares it to the DRL estimation. If there is a significant difference, Covy reinitializes its pose using AMCL coordinates. Comparing the two estimations frequently slows down the computation; therefore, this comparison happens every X steps (in our implementation every 20 steps).

4 EXPERIMENTAL EVALUATION

Covy’s vision and navigation systems are evaluated next.

4.1 Vision System

Two sets of experiments were conducted to evaluate Covy’s vision system: person’s location estimation accuracy and classification accuracy of breaches in social distancing. Each experiment was done in a simulated and real environment. For the person’s location estimation, we moved the person away from the camera by 1 m for every new experiment and took 50 pictures at each location. Additionally, we sampled a few other coordinates by moving the pedestrian vertically by 0.8 m. We repeated this experiment until the camera could not detect any pedestrian, which resulted in ranges of 23 and 16 m for the RGB camera and 5 and 7 m for the RGB-D camera in the simulated and real environment, respectively. The red circles in Figure 6 show the exact coordinates at which a person stood. For the breach detection accuracy, we placed two people at various coordinates in the scene while ensuring they were in the camera’s field of view and took 50 pictures at each location. To get balanced data, we ensured that they breached the social distancing rule in half of the experiment trials. For detecting people using the RGB-D camera, we used the YOLOv3 model [38] trained on the COCO dataset [29]. For the RGB-based detection, we used the MonoLoco model [6], trained on the KITTI dataset [16]. Finally, we profiled the execution of these algorithms the Jetson Nano and Jetson Xavier NX processor.

4.1.1 Localization. Figure 7 shows the average localization error (ALE) of Covy’s vision RGB-D and RGB localization methods. Two main conclusions we drew from these results are as follows.

First, from Figure 7a and 7c, we observe that there is a noticeable difference in the ALE patterns of the simulated and physical RGB-D camera. We conjecture that this discrepancy is due to the difficulty of simulating how the Intel RealSense camera [21] estimates depth. It uses active illumination for measuring distances to objects. Precise simulation

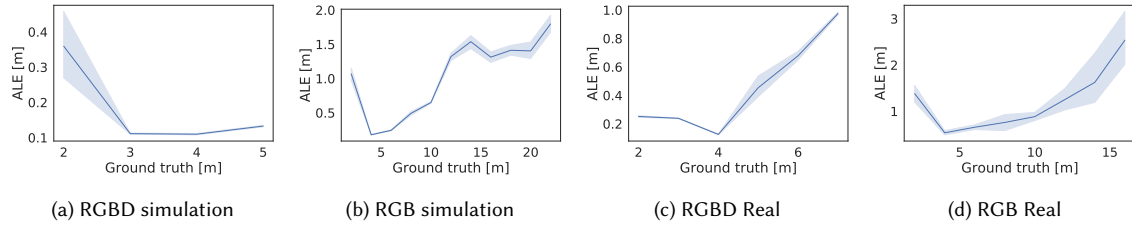


Fig. 7. Average localization error (ALE) with confidence interval as a function of distance – RGBD and RGB based system.

of active illumination requires accurate ambient light simulation which is hard. On the other hand, the results of the simulated and real RGB camera are more consistent (Figures 7b and 7d). This is expected as the input to both is a pure RGB image.

Second, when assessing the ALE in Figure 7c, we notice that the RGB-D camera can detect pedestrians standing at less than 5 m with an ALE < 0.4 m. The RGB system, however, reaches its minimum ALE of ≈ 0.4 m at 5 m and then the error goes up again to an average of ≈ 2.5 m at 16 m (7d). Furthermore, the variation in the coordinates estimation of the RGB method is higher than that of the RGB-D one. Consequently, Covy is less certain about the locations of faraway people; but, the accuracy increases as the distance between Covy and people shrinks. In conclusion, at short distances, i.e. ≤ 5 m, the RGB-D detection algorithm is the preferred choice, while from 5 m onwards, the RGB detection method is a better fit. Covy capitalizes on both to detect breaches up to 16 m away and approach the offenders safely.

4.1.2 Breaches Classification Accuracy. This experiment compares the performance of the RGB-D and RGB-based vision systems in detecting social distancing violations. We treat this problem as a binary classification task and evaluate the detection accuracy, recall, and precision. Figure 9 shows the confusion matrices of the classification, and Table 2 compares the said metrics between the two methods.

Simulation:- From Table 2, we notice that the accuracy is equal to 96% and 92% for the RGB-D and RGB systems with high precision and recall. Both methods can therefore accurately classify social distancing breaches in simulation. However, the recall of the RGB method is lower than that of the RGB-D one by 7%. In other words, the RGB vision system classifies more breaches as safe compared to the RGB-D counterpart. The reason is that, the RGB system has about three times the detection range of the RGB-D camera but the variance in the localization error increases significantly for large distances (> 13 m, Figure 7b). Hence, when running the experiments, we noticed that a large number of false negatives were detected for distances above 15 m.

Reality:- Similarly, the classification precision is high in the real environment ($\geq 90\%$) (Table 2). However, the accuracy and recall fall off. This decrease is due to the negative effect of the real environment and its surrounding on the performance of our systems. Additionally, we noticed, during the experiments, that many misclassifications happen at the limits of the cameras' field of view (i.e., where the ALE is high). Overall, both algorithms maintained accuracy of 82% in realistic conditions. Qualitative results of both methods are shown in Figure 8. Combined, these results show the promising ability of Covy in recognizing breaches in social distancing.

4.1.3 Hardware Performance. To analyze the computational resources utilization of the RGB and RGB-D methods, we profiled their execution on Jetson Nano and Jetson Xavier NX. We measured the CPU, GPU, and memory usage as shown in Table 3. For each iteration, we measured resource utilization at idle conditions, run the model for a few minutes to let it reach its steady-state conditions, and then took 100 measurements.

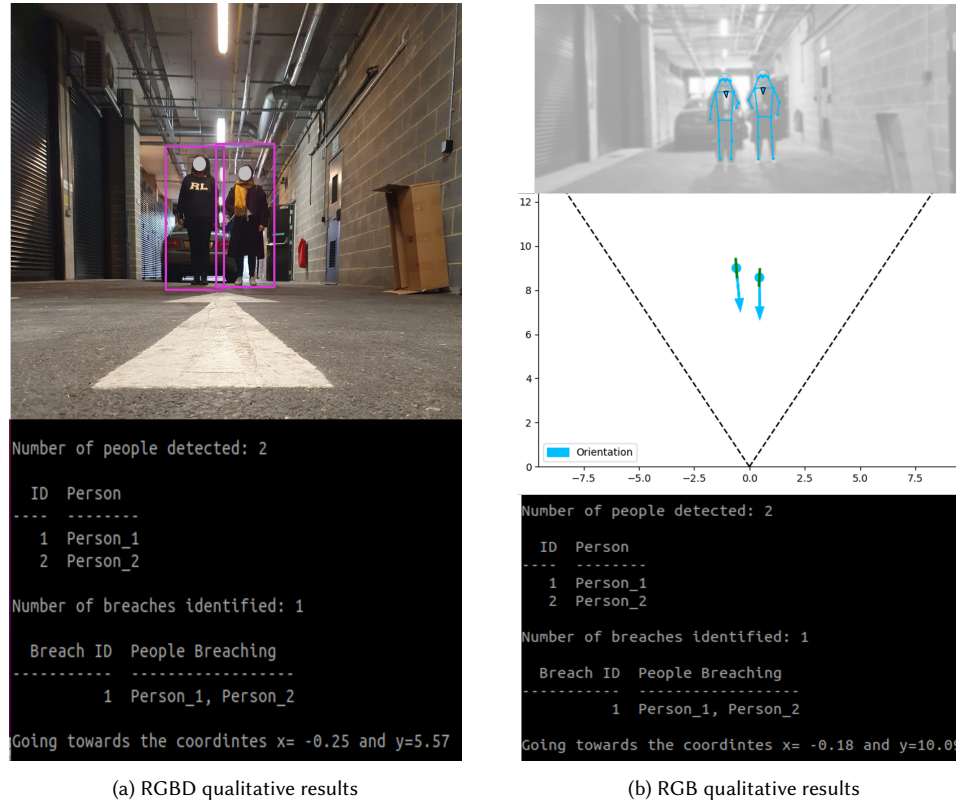


Fig. 8. Example of Covy's vision modules (i.e., RGB and RGB-D) and detection accuracy of breaches.

Method	Accuracy (%)	Precision (%)	Recall (%)	Environment
RGB-D	96	98	95	Simulation
RGB	92	96	88	Simulation
RGB-D	82	90	72	Reality
RGB	82	93	70	Reality

Table 2. Accuracy of classifying social distancing breaches

Jetson Nano was able to run the RGB-D detection system based on Yolov3 [38], but reached maximum CPU utilization ($\approx 99\%$) and very high GPU utilization (83%). Moreover, Jetson Nano was unable to run the resource-intensive RGB-based detection algorithm which runs multiple deep learning models to estimate the 3D coordinates of people in the scene.

Jetson Xavier NX, on the other hand, was able to run both systems with acceptable resource utilization. The RGB-based detection method noted the highest GPU utilization (59%), while the RGB-D system showed the highest CPU usage (65%). However, the memory consumption of the RGB system was high, averaging 7.2 GB of RAM out of the total 8.

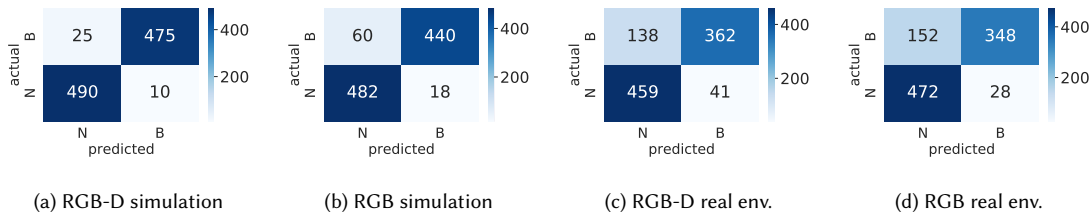


Fig. 9. Accuracy in Detection of Breaches Using Covy’s Vision Modules (RGB and RGB-D) in simulated and real environment. N: no breaches and B: breaches.

Hardware	Status	CPU1(%)	CPU2(%)	CPU3(%)	CPU4(%)	Memory (GB)	GPU(%)
Nano	Idle	18	15	15	14	1.6/4.1	3
	RGB detection	NA	NA	NA	NA	NA	NA
	RGB-D detection	99	98	99	99	2.7/4.1	83
Xavier NX	Idle	15	15	13	13	2.5/8	1
	RGB detection	44	42	36	34	7.2/8	59
	RGB-D detection	60	50	56	65	3.3/8	15
	Covy’s vision	76	63	70	75	7.4/8	63

Table 3. Performance comparison of breach detection algorithms on different hardware.

Considering that the individual performances were favorable, we tested Covy’s vision algorithm as a whole on Jetson Xavier NX. The overall performance seemed promising, with average utilization of 70%, 63%, and 92% of the CPU, GPU, and RAM, respectively.

4.2 Navigation

We evaluated the performance of the navigation stacks using success rate, failure rate due to collides or deadlocks, and average speed.

4.2.1 Experiment setup. We trained the DRL models on a computer equipped with an NVIDIA GeForce GTX 1060, 16 GB of RAM, and an Intel Core i7-8750H processor. We used the three virtual environments shown in Figure 10, to train and test our DRL algorithms using the Jetbot robot model. The environments consist of a 4×4 m² room-like environment with no obstacles, static obstacles, and dynamic obstacles. The DRL models are trained for 4000 episodes by navigating a Jetbot robot model in these environments. We tested the models capabilities in simulation and reality by sampling 35 random configurations for each environment type.

4.2.2 Training. Figure 11 shows the cumulative rewards obtained by DDPG and SAC during training in an environment with static and dynamic obstacles where each data point represents the average reward over 25 episodes. After ≈ 350 episodes, SAC surpasses DDPG in performance constantly. SAC reached a maximum average reward of approximately 3000, double that of the DDPG agent. We hypothesize that as SAC is a stochastic policy, it is able to explore the environment better and therefore collect higher rewards.

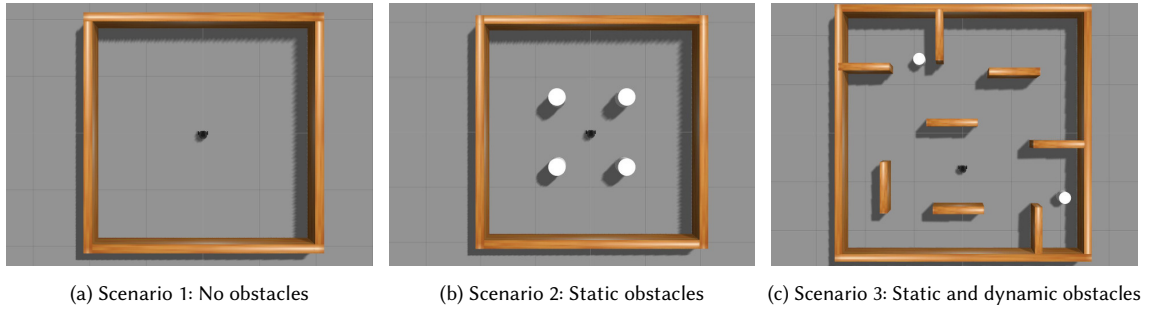


Fig. 10. Training environments.

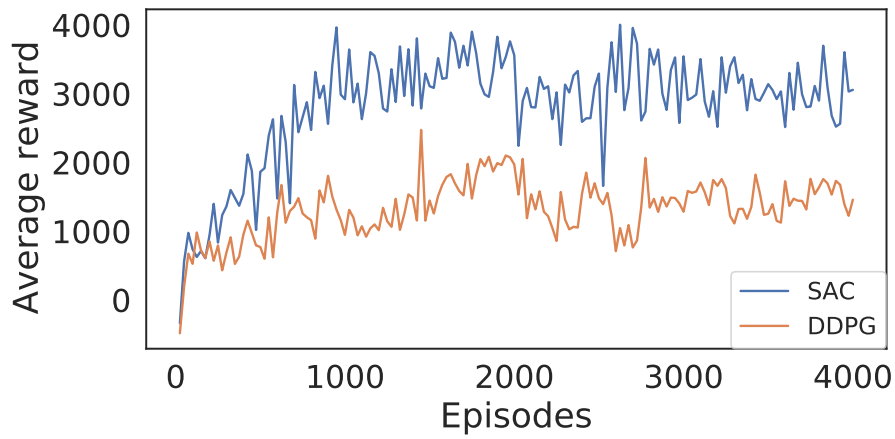


Fig. 11. Training in environment with varying obstacles.

Table 4. Comparison of the three navigation stacks in simulated and real environments.

Env.	Algorithms	Success (%)	Failures (collisions / deadlocks) (%)	Average Speed [m/s]
Simulation	DDPG	87	13 (8 / 5)	0.125
	SAC	92	8 (6 / 2)	0.17
	Hybrid navigation	93	7 (7 / 0)	0.046
Reality	DDPG	74	26 (11 / 15)	0.099
	SAC	80	20 (8 / 12)	0.13
	Hybrid navigation	90	10 (10 / 0)	0.057

4.2.3 *Navigation Accuracy.* Table 4 shows that the three navigation stacks are performant in simulation with a minimum success rate of $\geq 87\%$. However, in reality the performances drop by more than 10% for pure DRL approaches and by 3% for the hybrid navigation stack. On the other hand, the hybrid stack is about 2 to 3 times slower than its DRL counterparts. This is expected as the robot needs to keep track of its position on the given map. Furthermore, we see

that the SAC model performs better than the DDPG model in the real and simulated environment. Additionally, SAC is faster than DDPG in reaching the target: we suspect that the stochastic nature of SAC provides better exploration and allows the model to find more optimal paths than DDPG, which is a deterministic DRL agent. Contrary to the hybrid approach, both DDPG and SAC can get lost (or end up in a deadlock) in both environments. We conjecture that this is due to the use of LiDAR odometry which can produce inconsistent measurement when the robot moves fast. Overall, our hybrid approach performs the best the cost of slower navigation.

5 CONCLUSION AND FUTURE WORK

Covy is a robot designed to test a compound vision system and different navigation stacks. The target application is to promote social distancing practice during a pandemic (e.g., COVID-19). The vision algorithm that Covy uses extends the range of depth of the Intel RealSense D435i camera from an effective range of 6 m to 16 m. Covy navigates its surroundings autonomously using a hybrid navigation stack that combines a DRL agent with the probabilistic localization method AMCL. Results from navigating in realistic and simulated environments show that Covy's hybrid navigation stack is superior to a pure DRL-based one.

To further reduce the costs, next, we are planning to drop the LiDAR and develop a vision-based navigation stack. Then, a swarm of Covy robots shall be developed to target applications such as alerting littering individuals or finding objects of interest in airports or alike environments.

REFERENCES

- [1] Pranav Adarsh, Pratibha Rathi, and Manoj Kumar. 2020. YOLO v3-Tiny: Object Detection and Recognition using one stage improved model. In *2020 6th International Conference on Advanced Computing and Communication Systems (ICACCS)*. 687–694. <https://doi.org/10.1109/ICACCS48705.2020.9074315>
- [2] Imran Ahmed, Misbah Ahmad, Joel Rodrigues, Gwanggil Jeon, and Sadia Din. 2020. A deep learning-based social distance monitoring framework for COVID-19. *Sustainable Cities and Society* 65 (11 2020), 102571. <https://doi.org/10.1016/j.scs.2020.102571>
- [3] Merihan Alhafnawi, Edmund R Hunt, Severin Lemaignan, Paul O'Dowd, and Sabine Hauert. 2022. MOSAIX: a Swarm of Robot Tiles for Social Human-Swarm Interaction. In *2022 International Conference on Robotics and Automation (ICRA)*. IEEE, 6882–6888.
- [4] AMCL ROS: Adaptive Monte Carlo Localization ROS package. 2022. <http://wiki.ros.org/amcl>.
- [5] Lorenzo Bertoni, Sven Kreiss, and Alexandre Alahi. 2019. Monoloco: Monocular 3d pedestrian localization and uncertainty estimation. In *Proceedings of the IEEE/CVF International Conference on Computer Vision*. 6861–6871.
- [6] Lorenzo Bertoni, Sven Kreiss, and Alexandre Alahi. 2021. Perceiving Humans: from Monocular 3D Localization to Social Distancing. (2021). arXiv:2009.00984 [cs.CV]
- [7] Alex Bewley, Zongyuan Ge, Lionel Ott, Fabio Ramos, and Ben Uppcroft. 2016. Simple online and realtime tracking. *2016 IEEE International Conference on Image Processing (ICIP)* (Sep 2016). <https://doi.org/10.1109/icip.2016.7533003>
- [8] Nicolas Bredeche and Nicolas Fontbonne. 2022. Social learning in swarm robotics. *Philosophical Transactions of the Royal Society B* 377, 1843 (2022), 20200309.
- [9] Asma Channa, Nirvana Popescu, Justyna Skibinska, and Radim Burget. 2021. The rise of wearable devices during the COVID-19 pandemic: A systematic review. *Sensors* 21, 17 (2021), 5787.
- [10] Zhiming Chen, Tingxiang Fan, Xuan Zhao, Jing Liang, Cong Shen, Hua Chen, Dinesh Manocha, Jia Pan, and Wei Zhang. 2021. Autonomous social distancing in urban environments using a quadruped robot. *IEEE Access* 9 (2021), 8392–8403.
- [11] Youngjoon Choi, Miju Choi, Munhyang Oh, and Seongseop Kim. 2020. Service robots in hotels: understanding the service quality perceptions of human-robot interaction. *Journal of Hospitality Marketing & Management* 29, 6 (2020), 613–635.
- [12] Junior Costa de Jesus, Victor Kich, Alisson Kolling, Ricardo Grando, Marco Cuadros, and Daniel Fernando Gamarra. 2021. Soft Actor-Critic for Navigation of Mobile Robots. *Journal of Intelligent & Robotic Systems* 102 (06 2021). <https://doi.org/10.1007/s10846-021-01367-5>
- [13] Marco Dorigo, Guy Theraulaz, and Vito Trianni. 2021. Swarm robotics: past, present, and future [point of view]. *Proc. IEEE* 109, 7 (2021), 1152–1165.
- [14] Dieter Fox, Wolfram Burgard, Frank Dellaert, and Sebastian Thrun. 1999. Monte carlo localization: Efficient position estimation for mobile robots. *AAAI/IAAI* 1999, 343–349 (1999), 2–2.
- [15] Rubén Martín García, Daniel Hernández de la Iglesia, Juan F de Paz, Valderi RQ Leithardt, and Gabriel Villarrubia. 2021. Urban Search and Rescue with Anti-pheromone Robot Swarm architecture. In *2021 Telecoms Conference (ConfTELE)*. IEEE, 1–6.
- [16] Andreas Geiger, Philip Lenz, Christoph Stiller, and Raquel Urtasun. 2013. Vision meets Robotics: The KITTI Dataset. *International Journal of Robotics Research (IJRR)* (2013).

- [17] Tuomas Haarnoja, Aurick Zhou, Pieter Abbeel, and Sergey Levine. 2018. Soft actor-critic: Off-policy maximum entropy deep reinforcement learning with a stochastic actor. In *International conference on machine learning*. PMLR, 1861–1870.
- [18] Tuomas Haarnoja, Aurick Zhou, Kristian Hartikainen, George Tucker, Sehoon Ha, Jie Tan, Vikash Kumar, Henry Zhu, Abhishek Gupta, Pieter Abbeel, et al. 2018. Soft actor-critic algorithms and applications. *arXiv preprint arXiv:1812.05905* (2018).
- [19] Kaiming He, Georgia Gkioxari, Piotr Dollár, and Ross Girshick. 2017. Mask r-cnn. In *Proceedings of the IEEE international conference on computer vision*. 2961–2969.
- [20] Hen-Wei Huang, peter chai, Claas Ehmke, Gene Merewether, Fara Dadabhoy, Annie Feng, Akhil John Thomas, Canchen Li, Marco da Silva, Marc H Raibert, et al. 2020. Agile mobile robotic platform for contactless vital signs monitoring. (2020).
- [21] Intel RealSense D435i Depth Camera 2021. Intel. <https://www.intel.com/content/www/us/en/architecture-and-technology/realsense-overview.html>.
- [22] Jetbot: An AI-Driven Robot. 2021. Waveshare. <https://www.waveshare.com/jetbot-ai-kit.htm>.
- [23] Gregory Kahn, Adam Villaflor, Bosen Ding, Pieter Abbeel, and Sergey Levine. 2018. Self-supervised deep reinforcement learning with generalized computation graphs for robot navigation. In *2018 IEEE International Conference on Robotics and Automation (ICRA)*. IEEE, 5129–5136.
- [24] Shinji Kawakura and Ryosuke Shibasaki. 2020. Deep Learning-Based Self-Driving Car: JetBot with NVIDIA AI Board to Deliver Items at Agricultural Workplace with Object-Finding and Avoidance Functions. *European Journal of Agriculture and Food Sciences* 2, 3 (2020).
- [25] Sven Kreis, Lorenzo Bertoni, and Alexandre Alahi. 2019. Pifpaf: Composite fields for human pose estimation. In *Proceedings of the IEEE/CVF conference on computer vision and pattern recognition*. 11977–11986.
- [26] Jonáš Kulhánek, Erik Derner, and Robert Babuška. 2021. Visual navigation in real-world indoor environments using end-to-end deep reinforcement learning. *IEEE Robotics and Automation Letters* 6, 3 (2021), 4345–4352.
- [27] Jonáš Kulhánek, Erik Derner, Tim De Bruin, and Robert Babuška. 2019. Vision-based navigation using deep reinforcement learning. In *2019 European Conference on Mobile Robots (ECMR)*. IEEE, 1–8.
- [28] Timothy P Lillicrap, Jonathan J Hunt, Alexander Pritzel, Nicolas Heess, Tom Erez, Yuval Tassa, David Silver, and Daan Wierstra. 2015. Continuous control with deep reinforcement learning. *arXiv preprint arXiv:1509.02971* (2015).
- [29] Tsung-Yi Lin, Michael Maire, Serge Belongie, Lubomir Bourdev, Ross Girshick, James Hays, Pietro Perona, Deva Ramanan, C. Lawrence Zitnick, and Piotr Dollár. 2015. Microsoft COCO: Common Objects in Context. *arXiv:1405.0312* [cs.CV]
- [30] Pinxin Long, Tingxiang Fan, Xinyi Liao, Wenxi Liu, Hao Zhang, and Jia Pan. 2018. Towards optimally decentralized multi-robot collision avoidance via deep reinforcement learning. In *2018 IEEE International Conference on Robotics and Automation (ICRA)*. IEEE, 6252–6259.
- [31] Abraham Lopez-Lora, Pedro J Sanchez-Cuevas, Alejandro Suárez, A Garofano-Soldado, Anibal Ollero, and Guillermo Heredia. 2020. MHYRO: Modular HYbrid ROBOT for contact inspection and maintenance in oil & gas plants. In *2020 IEEE/RSJ International Conference on Intelligent Robots and Systems (IROS)*. IEEE, 1268–1275.
- [32] Zhihan Lv, Jaime Lloret Mauri, and Houbing Song. 2020. Editorial RGB-D sensors and 3D reconstruction. *IEEE Sensors Journal* 20, 20 (2020), 11751–11752.
- [33] Amjad Yousef Majid, Serge Saaybi, Tomas van Rietbergen, Vincent Francois-Lavet, R Venkatesha Prasad, and Chris Verhoeven. 2021. Deep Reinforcement Learning Versus Evolution Strategies: A Comparative Survey. *arXiv preprint arXiv:2110.01411* (2021).
- [34] Chiranjivi Neupane, Anand Koirala, Zhenglin Wang, and Kerry Brian Walsh. 2021. Evaluation of depth cameras for use in fruit localization and sizing: Finding a successor to kinect v2. *Agronomy* 11, 9 (2021), 1780.
- [35] Narinder Singh Punj, Sanjay Kumar Sonbhadra, Sonali Agarwal, and Gaurav Rai. 2020. Monitoring COVID-19 social distancing with person detection and tracking via fine-tuned YOLO v3 and Deepsort techniques. *arXiv preprint arXiv:2005.01385* (2020).
- [36] Morgan Quigley, Ken Conley, Brian Gerkey, Josh Faust, Tully Foote, Jeremy Leibs, Rob Wheeler, and Andrew Ng. 2009. ROS: an open-source Robot Operating System. *ICRA Workshop on Open Source Software* 3.
- [37] Adhiti Raman, Venkat Krovi, and Matthias Schmid. 2018. Empowering Graduate Engineering Students With Proficiency in Autonomy. V05AT07A080.
- [38] Joseph Redmon and Ali Farhadi. 2018. Yolov3: An incremental improvement. *arXiv preprint arXiv:1804.02767* (2018).
- [39] Mahdi Rezaei and Mohsen Azarmi. 2020. DeepSOCIAL: Social Distancing Monitoring and Infection Risk Assessment in COVID-19 Pandemic. *Applied Sciences* 10, 21 (Oct 2020), 7514. <https://doi.org/10.3390/app10217514>
- [40] Mahdi Rezaei and Mohsen Azarmi. 2020. DeepSOCIAL: Social Distancing Monitoring and Infection Risk Assessment in COVID-19 Pandemic. *Applied Sciences* 10, 21 (Oct 2020), 7514. <https://doi.org/10.3390/app10217514>
- [41] RPLidar A2: a Laser Range Scanner. 2021. Slamtec. <https://www.slamtec.com/en/Lidar/A2>.
- [42] Stuart J Russell. 2010. *Artificial intelligence a modern approach*. Pearson Education, Inc.
- [43] Adarsh Jagan Sathyamoorthy, Utsav Patel, Yash Ajay Savle, Moumita Paul, and Dinesh Manocha. 2020. COVID-Robot: Monitoring Social Distancing Constraints in Crowded Scenarios. *CoRR* (2020).
- [44] John Schulman, Filip Wolski, Prafulla Dhariwal, Alec Radford, and Oleg Klimov. 2017. Proximal policy optimization algorithms. *arXiv preprint arXiv:1707.06347* (2017).
- [45] Francesco Setti, Chris Russell, Chiara Basseti, and Marco Cristani. 2015. F-formation detection: Individuating free-standing conversational groups in images. *PloS one* 10, 5 (2015), e0123783.
- [46] Yang Shen, Dejun Guo, Fei Long, Luis A Mateos, Houzhu Ding, Zhen Xiu, Randall B Hellman, Adam King, Shixun Chen, Chengkun Zhang, et al. 2020. Robots under COVID-19 pandemic: A comprehensive survey. *Ieee Access* (2020).
- [47] Stereolabs 2022. ZED 2: An AI Stereo Camera. <https://www.stereolabs.com/zed-2i/>.

- [48] Chanjuan Sun and Zhiqiang Zhai. 2020. The efficacy of social distance and ventilation effectiveness in preventing COVID-19 transmission. *Sustainable Cities and Society* 62 (2020), 102390. <https://doi.org/10.1016/j.scs.2020.102390>
- [49] Shaoxiong Sun, Amos A Folarin, Yatharth Ranjan, Zulqarnain Rashid, Pauline Conde, Callum Stewart, Nicholas Cummins, Faith Matcham, Gloria Dalla Costa, Sara Simblett, and et al. 2020. Using Smartphones and Wearable Devices to Monitor Behavioral Changes During COVID-19. *Journal of Medical Internet Research* 22, 9 (Sep 2020), e19992. <https://doi.org/10.2196/19992>
- [50] Hartmut Surmann, Christian Jestel, Robin Marchel, Franziska Musberg, Housseem Elhadj, and Mahbube Ardani. 2020. Deep reinforcement learning for real autonomous mobile robot navigation in indoor environments. *arXiv preprint arXiv:2005.13857* (2020).
- [51] Lei Tai, Giuseppe Paolo, and Ming Liu. 2017. Virtual-to-real deep reinforcement learning: Continuous control of mobile robots for mapless navigation. In *2017 IEEE/RSJ International Conference on Intelligent Robots and Systems (IROS)*. IEEE, 31–36.
- [52] Zoltán Voko and Janos Pitter. 2020. The effect of social distance measures on COVID-19 epidemics in Europe: an interrupted time series analysis. *GeroScience* 42 (06 2020). <https://doi.org/10.1007/s11357-020-00205-0>
- [53] Nicolai Wojke, Alex Bewley, and Dietrich Paulus. 2017. Simple Online and Realtime Tracking with a Deep Association Metric. arXiv:1703.07402 [cs.CV]
- [54] Jiaqi Xiang, Qingdong Li, Xiwang Dong, and Zhang Ren. 2019. Continuous control with deep reinforcement learning for mobile robot navigation. In *2019 Chinese Automation Congress (CAC)*. IEEE, 1501–1506.